

Mesoscopic Fibrillation Properties of Pressure Sensitive Adhesives Based on Latex Films

Tatiana D. Dimitrova,[†] Diethelm Johannsmann,^{*,†} Norbert Willenbacher,[‡] and Andreas Pfau[‡]

Max-Planck-Institute for Polymer Research, Ackermannweg 10, D-55128 Mainz, Germany, and BASF Aktiengesellschaft, Polymer Physics, 67056 Ludwigshafen, Germany

Received January 22, 2003. In Final Form: April 15, 2003

Slow pulling experiments with atomic force microscope (AFM) tips were performed on industrial acrylic latices, where the Brownian motion of the tip was monitored in parallel to the static force. From the noise power spectra of the tip's thermal motion, one can infer the effective spring constant and the drag coefficient of the tip–sample system. The results from AFM pulling experiments correlate well with macroscopic tack tests performed on the same materials at comparable stress levels. The fraction of “successful pulls”, meaning pulls where an extended loop of adhesion hysteresis forms, decreases with aging. Presumably, the internal cohesion of the material increases as film formation proceeds, such that the formation of cusps or tip-induced deformations of the surface becomes less likely. For the most tacky material, the formation of a continuous film was incomplete even after 6 months of storage. The successful pulls are characterized by a discrete number of steps in both static force and the spring constant. The steps are attributed to the rupture events occurring inside the film. Internal heterogeneity has an influence on the tack.

Introduction

Adhesion and controlled loss of adhesion are processes of great importance in everyday life and technology. Especially when polymers are part of the picture, adhesion is a rather complicated phenomenon, involving wetting, diffusion, plastic flow on different length scales, chain disentanglement, chain scission, and various elastic instabilities.¹ For elastomers, a popular starting point for modeling is the Johnson, Kendall, and Roberts (JKR) theory.² The JKR model makes a statement about the radius of contact and the adhesion hysteresis when a soft sphere is pushed against a solid substrate. It assumes a small contact area, flat surfaces, and linear elasticity. Shull has reviewed the use of the JKR model and various extensions.³

Some important properties of pressure sensitive adhesives (PSAs) are not captured by the JKR theory because the separation process involves plastic flow.⁴ The total energy of separation can be orders of magnitude larger than the equilibrium surface energy due to the large amount of energy dissipated during flow. The dissipated energy is often measured in a “tack test”, where a cylindrical or spherical probe of some millimeters in diameter is brought into contact with the sample and subsequently withdrawn.⁵ The force–distance curves usually show an initial peak and an extended tail, the latter being caused by the formation of “filaments”. The energy of separation is the integral over the force–distance curve. A large energy of separation is one of the performance parameters of industrial PSAs. Zosel has reported on the special rheological properties of bulk polymers

which have good performance in tack tests.⁵ It turns out that an optimum degree of cross linking, resulting in a “critical gel behavior”, is rather essential. By proper choice of the microgel content, one can tailor the viscoelastic behavior to achieve a proper balance between cohesive and adhesive strength of the film.

On the microscopic scale, the forces of adhesion and the energy of separation have gained much attention in the context of single-molecule force spectroscopy.^{6,7} When the force–distance curve shows complex patterns (like a sawtooth pattern), these specific features are related to intramolecular transitions of shape.^{6–8} It has been argued that such a sawtooth may be the result of an evolutionary optimization process. From a mechanical point of view, it is not clear why a sawtooth pattern should be optimal. While the energy of adhesion certainly is large, the elastic instabilities would induce an irregular motion, which is undesired in most engineering environments.

The mesoscopic scale has been investigated to a lesser extent. Given that many technical materials have a granular structure, interactions on the micron scale should be of high importance. Presumably, the distinct patterns occurring in the force–distance curves of certain complex molecules are smeared out on the micron scale due to ensemble averaging. Still, it is expected that the force–distance curves acquired with micron-sized probes (here atomic force microscope (AFM) tips) are different from the outcome of the tack tests. Exploring the scale dependence of tack tests can shed light on the mechanisms of energy dissipation, which are so important in practice.

Several researchers have worked on the mechanics of individual latex spheres. For example, Routh and Russel consider the deformation and further collapse of two spheres (both viscoelastic) as a function of the rheological properties of the surrounding medium.⁹ They introduce three dimensionless parameters, the values of which determine the scenario of the film formation. Their

* To whom correspondence should be addressed. Present address: Institute of Physical Chemistry, Arnold-Sommerfeld Str. 4, D-38687 Clausthal-Zellerfeld, Germany. Phone: +49-5323-723768. Fax: +49-5323-724835. E-mail: johannsmann@pc.tu-clausthal.de.

[†] Max-Planck-Institute for Polymer Research.

[‡] BASF Aktiengesellschaft.

(1) Brown, H. R. *Annu. Rev. Mater. Sci.* **1991**, *21*, 463.

(2) Johnson, K. L.; Kendall, K.; Roberts, A. D. *Proc. R. Soc. London* **1971**, *A324*, 301.

(3) Crosby, A. J.; Shull, K. R.; Lakrout, H.; Creton, C. *J. Appl. Phys.* **2000**, *88*, 2956.

(4) Crosby, A. J.; Shull, K. R. *J. Polym. Sci., Part B: Polym. Phys.* **1999**, *37*, 3455.

(5) Zosel, A. *J. Adhes.* **1994**, *44*, 1.

(6) Haupt, B. J.; Senden, T.; Sevick, E. M. *Langmuir* **2002**, *18*, 2174.

(7) Hugel, T.; Grosholz, M.; Clausen-Schaumann, H.; Pfau, A.; Gaub, H.; Seitz, M. *Macromolecules* **2001**, *34*, 1039.

(8) Marszalek, P. E.; Oberhauser, A. F.; Pang, Y.-P.; Fernandez, J. M. *Nature* **1998**, *396*, 661.

(9) Routh, A. F.; Russel, W. B. *Langmuir* **1999**, *15*, 7762.

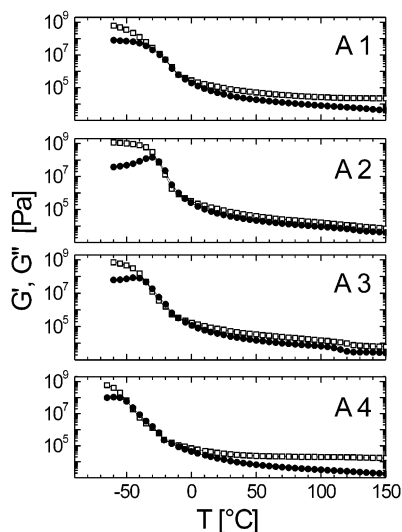


Figure 1. Surface rheological properties of the studied films: (□) storage modulus, G' ; (●) loss modulus, G'' .

analysis holds for temperatures not much higher than the glass transition temperature T_g and correlates reasonably well with the experimental data. Portigliatti et al.¹⁰ have also focused on individual latex spheres instead of single molecules. They obtained tapping-mode AFM images of isolated particles well above T_g before and after an “adhesion test”, which was performed by means of an AFM tip. Their experiments give evidence of a strong deformation of the latex particle after drawing a “nanofilament” from it.

One of the goals of this study was to elucidate the physical origin of tackiness in the case of particulate films. This required reducing the size of the probe body down to an AFM tip, so that an individual particle can be addressed. We used the AFM-based instrumentation as both imaging and manipulation tool. The AFM tip was driven interactively and used as a mesoscopic tack tester. Due to the mesoscopic nature of the probe, one can easily observe its Brownian motion. We exploit this advantage by performing AFM noise analysis in parallel to the pulling experiments. The noise power spectra¹¹ contain the spring constant and the drag coefficient of the tip–polymer interaction. This approach allows for dynamic mechanical spectroscopy in the kilohertz range in parallel to the classical force spectroscopy.

Experimental Section

Sample Preparation and Characterization. We report on four different polyacrylate dispersions from emulsion polymerization termed A1, A2, A3, and A4. These latices are commercial products from BASF Aktiengesellschaft especially developed for PSA applications. A1 is mainly used for self-adhesive tapes, A2 is designed for poly(vinyl chloride) (PVC) face materials, A3 for film labels, and A4 mainly for removable labels. The particle diameter for these materials is about 150–300 nm, and the solids content is 50% for sample A1, 55% for samples A2 and A4, and 60% for sample A3. Details of chemical composition and synthesis are proprietary to the manufacturer.

Figure 1 shows the temperature dependence of the storage modulus, G' , and loss modulus, G'' , at 1 Hz. The data were taken on 1 mm thick films in parallel-plate geometry (diameter, 8 mm), employing an ARES (Rheometrics Scientific Inc., USA) rheometer equipped with the force transducer 2KFRTN1 (torque range, 2

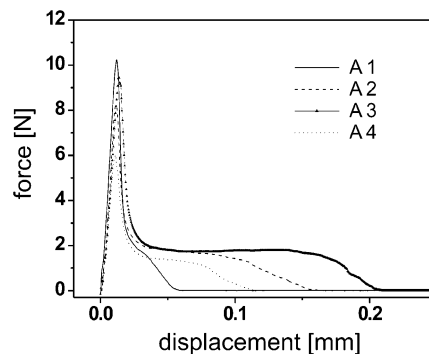


Figure 2. Tack curves of the studied films.

Table 1. Peak Force and Energy of Separation Obtained from Tack Tests

sample	peak force F_2 [N]	standard deviation F_2 [N]	energy of separation w [J m ⁻²]	standard deviation w [J m ⁻²]
A1	10.2	1.0	50	1.9
A2	8.2	1.2	86	6.5
A3	9.2	1.2	124	10.2
A4	5.3	0.7	54	1.4

$\times 10^{-6}$ to 0.2 Nm). As Figure 1 shows, all films have a T_g (defined here as the temperature where G'' has its maximum) much below room temperature. The detailed analysis gives $T_g = -40, -37, -40,$ and -55 °C for samples A1, A2, A3, and A4, respectively. All samples have a loss tangent $\tan \delta = G''/G' < 1$ even at the highest investigated temperature. For samples A1 and A4, this effect is particularly strong. These samples have a rather high content of cross-linked chains (microgels). Samples A2 and A3 have an extended range, where G' almost equals G' . This quasi-critical behavior is typical for dispersions optimized for PSA applications. Sample A3 shows a small step at 120 °C, which is possibly connected to a glass transition of the continuous phase.¹² The time–temperature superposition is valid for these acrylic polymers. Typically, a frequency shift of one decade is equivalent to a temperature shift of about 8 °C. Therefore, the rheological data taken at $f = 1$ Hz can be transformed to equivalent data for $f = 55$ kHz (the resonance frequency of the cantilever) by shifting along the temperature scale.

The glass substrates (standard microscope slides) were cleaned by 15 min of sonication in ionic detergent (2% Hellmanex, HELLMA, Germany), followed by 20 min of sonication in deionized water, washing with Milli-Q water, and drying in nitrogen. Films with a (wet) thickness of 20–30 microns were formed with a pulling blade (Erichsen, Germany; model 97065 or 94060). The samples were dried at room temperature for 24 h. The surface of the dried films was then gently washed with deionized water. After washing, the films were again dried for 24 h and stored desiccated. The aging of the films was achieved only by storage. The term “time after preparation” used below refers to the time elapsed after the second drying step. There is a possibility for surfactant migration toward the top of the film, thus influencing the pulling behavior.¹³ We checked this hypothesis on one of the systems, washing additionally the surface prior to pulling experiments. No difference was observed.

The tack curves were obtained by means of a home-built setup, operating with a stainless steel cylindrical probe, 2 mm in diameter. The probe was brought in contact with the film for 1 s at a loading force of 0.5 N and then retracted at a constant velocity of 1 mm/s. Figure 2 shows representative tack curves. The adhesion energy is defined as the area under the load–displacement curve, normalized by the initial contact area. At least 10 tack curves were averaged to obtain the peak force and the separation energy listed in Table 1. From Figure 2 and Table 1, one deduces that A3 is the most tacky material, followed by A2.

(10) Portigliatti, M.; Koutsos, V.; Hervet, H.; Léger, L. *Langmuir* **2000**, *16*, 6374.

(11) Roters, A.; Johannsmann, D. *J. Phys.: Condens. Matter* **1996**, *8*, 7561.

(12) Ferry, J. D. *Viscoelastic properties of polymers*; Wiley and Sons: New York, 1980.

(13) Kientz, E.; Holl, Y. *Colloids Surf., A* **1993**, *78*, 255.

AFM micrographs were taken with a NanoScope III atomic force microscope (Digital Instruments, Inc., Santa Barbara, CA) equipped with a J-scanner. All films were imaged in air at room temperature (22 °C) in Tapping Mode. We used Ultrasharp silicon probes (MikroMach, Estonia; model CSC12) with a resonant frequency of about 170 kHz and a spring constant (manufacturer information) of 1.75 N/m. In Tapping Mode (intermittent contact), the cantilever is oscillated near its resonance frequency, with an amplitude high enough to overcome the adhesive forces.¹⁴ The values for the amplitude set-point and engage set-point are given as Supporting Information. At least three images at randomly chosen locations were acquired for each film, keeping the parameters of the feedback constant.

The pulling experiments were performed with a Molecular Force Probe (MFP; Asylum Research, Santa Barbara, CA), equipped with commercial V-shaped Si₃N₄ cantilevers (Digital Instruments). The resonant frequency of the cantilevers was 56 kHz. The instrument allows for a z-range of 10 microns and has a possibility to drive the cantilever interactively. We “manually” approached the cantilever to the surface, which enabled us to detect the jump into contact without allowing the tip to penetrate further into the film. The investigated objects are picked up by the tip via unspecific adsorption. The AFM tip is then retracted away from the film in steps of 1 nm, thus stretching a small filament. A sketch of the experimental setup is provided as Supporting Information. At each step, the thermal vibration (Brownian motion) of the cantilever is recorded for a period of 0.2 s. The registration of the cantilever’s noise requires a disconnection of the feedback loop. This introduces drift in the time-averaged displacement of the cantilever and limits the spatial resolution to 1 nm. The micromechanical properties of the objects stretched between the tip and the film are extracted from the noise power spectra as described below and plotted against the travel of the z-piezo. Since the AFM does not allow for absolute distance measurements, we consider as “zero” the location where the filament is picked up and the retraction of the piezo away from the film begins. We name the objects “filaments” following the terminology of Portigliatti et al.¹⁰ and in analogy with the macroscopic fibrillation observed in tack or peel experiments. Note that our filaments are rather short (<1 μm).

In ambient conditions, the studied film is covered by a thin layer of water. This may affect the near-surface resonance properties of the cantilever in the very beginning of the pulling. Since the investigated filaments are hundreds of nanometers long, this effect is unimportant.

Data Analysis

AFM Noise Analysis. The technique of AFM noise analysis has been described in detail elsewhere.¹¹ Here we recall only the main points. We model the cantilever as an elastically suspended mass point, which experiences random forces from its environment. The statistical motion of such a particle is described by the Langevin equation:

$$m \frac{d^2 z(t)}{dt^2} + \xi \frac{dz(t)}{dt} + \kappa z(t) = R(t) \quad (1)$$

where $z(t)$ is the displacement, m is the effective mass, κ is the spring constant, ξ is the friction coefficient, and $R(t)$ is the random force. The noise power spectral density (PSD) of the cantilever motion¹¹ is given by resonance curves of the form

$$|\delta z^2(\omega)| = \frac{k_B T}{\pi m} \frac{\xi}{(\kappa - m\omega)^2 + \xi^2 \omega^2} = \frac{A\gamma}{(\omega_0^2 - \omega^2)^2 + \gamma^2 \omega^2} \quad (2)$$

where $k_B T$ is the thermal energy, ω_0 is the resonance frequency, γ is the width of the resonance, and A is the amplitude. In principle, one could fit a resonance curve

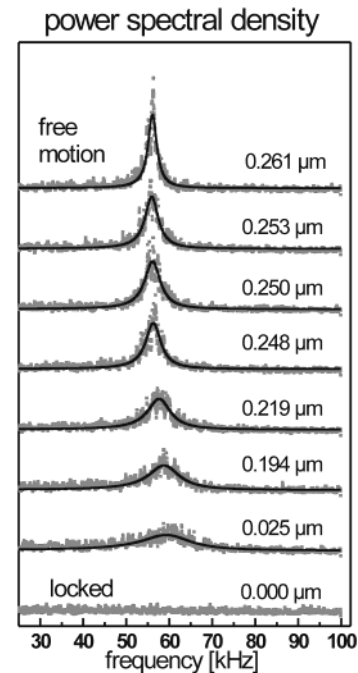


Figure 3. The noise power spectra (gray dots) and corresponding fits with resonance curves (lines) as the piezo travels away from the film. The curves are offset vertically for clarity.

to the data and calculate the mass, m , the drag coefficient, ξ , and the spring constant, κ , as $m = k_B T / (\pi A)$, $\xi = \gamma k_B T / (\pi A)$, and $\kappa = \omega_0^2 k_B T / (\pi A)$.

The frequency and the bandwidth are fitted with an accuracy of a few percent. However, it turned out that the amplitude A is determined with poor reproducibility due to a nonthermal noise floor in the spectra, which is of electronic origin. We therefore resort to another relation for the spring constant, which is the equipartition theorem:

$$\kappa_{eq} \cong \frac{k_B T}{\langle \delta z^2 \rangle} \quad (3)$$

The limited validity of eq 3 has been discussed in the literature extensively.¹⁵ The nonthermal noise floor also affects this calculation, but it does so in a reproducible way. While the absolute values of κ_{eq} may be disputable, variations of κ_{eq} are determined very reliably. Since changes of the spring constant induced by the sample are the goal of this investigation, we base our conclusions on κ_{eq} . Having determined κ_{eq} from the equipartition theorem, we calculate the friction coefficient, ξ , and the mass, m , as

$$\xi = \kappa_{eq} \frac{\gamma}{\omega_0^2} \quad (4)$$

$$m = \frac{\kappa_{eq}}{\omega_0^2}$$

Figure 3 shows typical power spectra (gray dots) and corresponding fits (lines) as a function of the piezo travel away from the film surface. The experiments were performed in air, where the resonances are rather sharp. The entire information is contained in the resonances. While the viscoelastic parameters, κ and ξ , can, in principle, depend on frequency, this effect remains without

(14) Sheiko, S. *Adv. Polym. Sci.* **2000**, *151*, 61.

(15) (a) Butt, H.-J.; Jaschke, M. *Nanotechnology* **1995**, *6*, 1. (b) Levy, R.; Maaloum, M. *Nanotechnology* **2002**, *13*, 33.

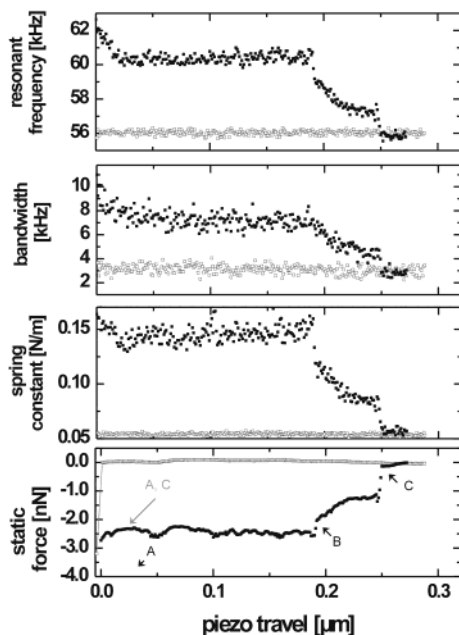


Figure 4. Successful (■) and unsuccessful (□) pulls. The letters indicate the attachment of the filament to the tip (A), the transformation(s) that the filament undergoes (B), and the detachment of the filament (C).

consequences for sharp resonances. Clearly, thermal excitation of the cantilever is possible only for soft surfaces. When the tip touches a hard surface or penetrates into the film, the effective spring constant becomes high, and the cantilever's mean square displacement drops to the level of the electronic background.

A fourth quantity which is automatically obtained is the static force, F_{stat} , calculated from the time-averaged displacement of the cantilever, $\langle z \rangle$. The force experiences a considerable drift because the feedback loop has to be disconnected and the total data acquisition time per filament on average was 10–15 min. Even so, the force discontinuities are reliably determined and we use them to detect the transitions, occurring during stretching of the filaments.

Results

Figure 4 shows the resulting fit parameters as a function of the piezo travel for two experiments with rather different outcomes. Both pulls were done on sample A2. The full dots correspond to an experiment where a filament has been successfully picked up. An adhesive force of about 2 nN develops. The maximal extension is about 250 nm which corresponds to the diameter of a single sphere. The energy of adhesion is about 5×10^{-16} J. This corresponds to an effective contact area of about 5 nm^2 if one applies the energy of separation determined by the macroscopic tack test (see Table 1) on the microscopic scale. The open symbols in Figure 4 correspond to what we call an "unsuccessful pull". The tip jumps out of contact right when the pull is initiated. All other parameters take the values of the free cantilever right then.

Since all the parameters extracted from the noise spectra reflect the entire system cantilever–filament, it is important to perform all experiments with *one and the same cantilever*. We occasionally checked by scanning electron microscopy that no residual material had accumulated on the cantilever. Whenever we checked, the polymer had completely detached from the cantilever.

Aging and Surface Morphology. The mechanisms of film formation have, for instance, been reviewed by

Keddie.¹⁶ Generally speaking, the process of film formation is believed to remove the boundaries between different latex particles and lead to the formation of a clear, homogeneous phase. One of the prerequisites of film formation is a low glass transition temperature of the polymer, allowing for deformation of the spheres and chain interdiffusion. Indeed, all dispersions investigated here have a T_g below -30 °C.

Interestingly, the AFM micrographs (Figure 5) show that in some cases the film formation is incomplete even after 6 months of storage. This phenomenon is most clearly visible for dispersion A3, which happens to be the tackiest material as well. We can only speculate which molecular parameters are essential for preventing complete coalescence. Presumably, a high stability of the membranes separating the particles helps. In this context, it seems interesting that the interparticle phase for sample A3 appears to have a glass transition of its own at $T \cong 120$ °C (cf. Figure 1).

In Figure 5, we present the evolution of the surface morphology of the studied films. Only the phase images are shown since they characterize the local viscosity of the film and can give evidence of phase separation even if the surface is perfectly flat. For the films made of A1 (first column), the image suggests some welding of the neighboring particles after 1 day of storage. The individual polymer particles are still distinguishable albeit deformed.

After 3 weeks of aging of these films, interparticle fusion develops; the image shows less structure, and one hardly recognizes individual particles any longer. After 6 months of storage, the spheres appear to have fused one into another. The top-left graph in Figure 6 represents the fraction of successful pulls with time.

The dispersions A2 and A3 (second and third columns in Figure 5) substantially differ from A1. One does not observe well-pronounced flattening and coalescence. Even after 6 months of storage, fusion of the lattices is incomplete. Mallegol and Keddie have observed the same phenomenon for acrylic latices of a similar type.¹⁷ Both films flatten with time, but the single spheres are clearly seen. For these two systems (A2 and A3), we generally observe a larger fraction of successful pulls than for the system A1 (Figure 6). Actually, the fraction of successful pulls decreases with time, giving further support to the hypothesis that partial coalescence is beneficial for tack. The last column in Figure 5 shows the surface morphology (phase image as well) of a film produced from the dispersion A4. In this case, the particles coalesce very well. Each surface particle is in contact with its neighbors via well-developed bridges that are clearly seen. The identity of the particles is completely lost after 6 months of storage. We were able to draw only very few filaments, the number of successful pulls being always less than 5% as shown in Figure 6.

A comparison of Figure 2 and Figure 6 suggests a correlation between mesoscopic and macroscopic measurements. The higher the likelihood of drawing a filament upon a gentle contact of the AFM tip with the film, the tackier the material (where tack is quantified by the area under the curve, not the peak force). Note that such a correlation is not necessarily expected. One could very well argue that tack is much affected by internal cohesion, whereas the AFM measures adhesion. However, in the mode employed here, the AFM probes not only adhesion but near-surface internal cohesion between the particles as well.

(16) Keddie, J. L. *Mater. Sci. Eng. Rep.* **1997**, *21*, 101.

(17) Mallegol, J.; Dupont, O.; Keddie, J. L. *Langmuir* **2001**, *17*, 7022.

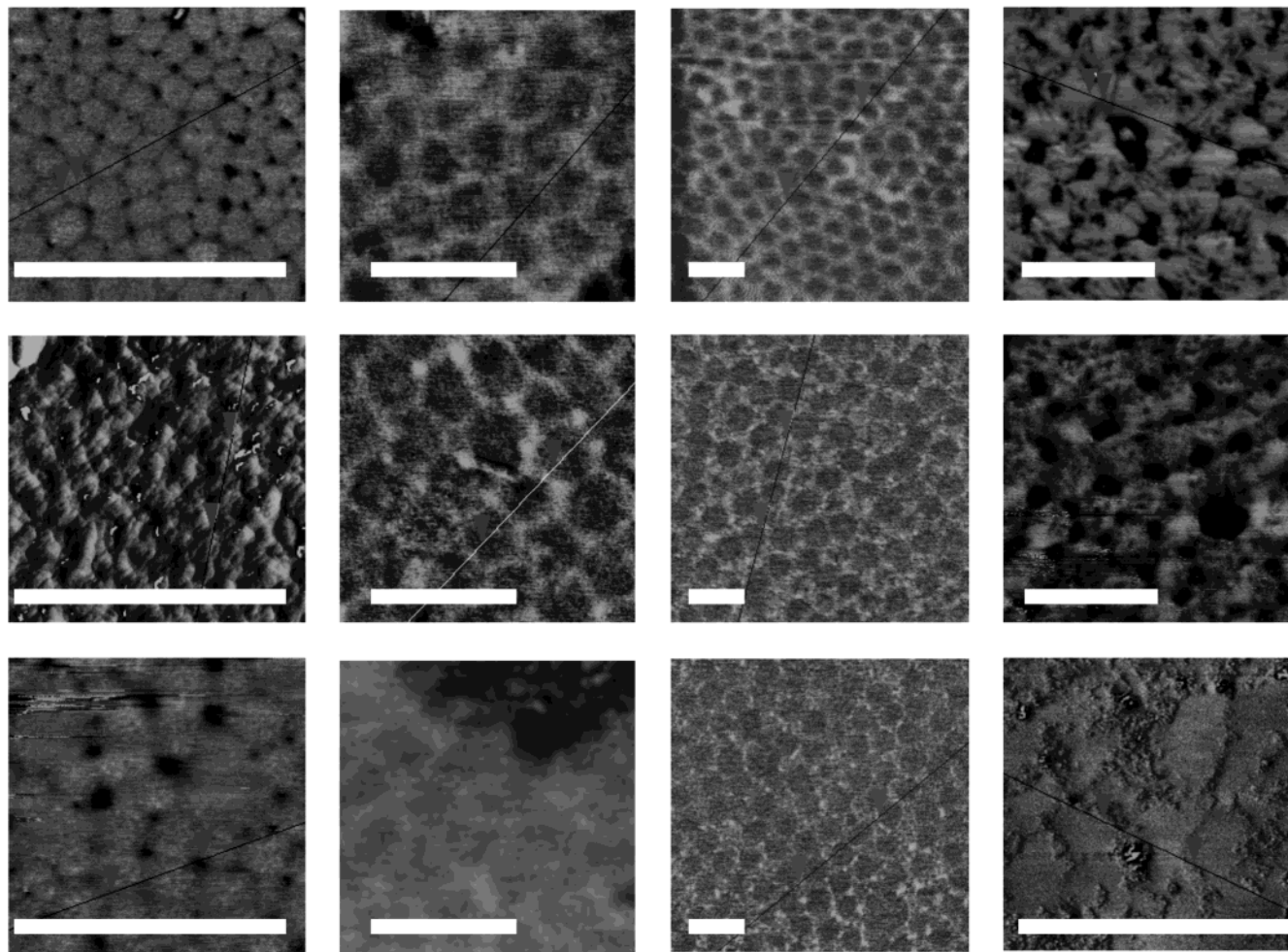


Figure 5. Evolution of the surface morphology (phase contrast Tapping Mode imaging). From left to right: A1, A2, A3, and A4. From top to bottom: 1 day after preparation, 3 weeks after preparation, and 6 months after preparation. The bar corresponds to 1 micron.

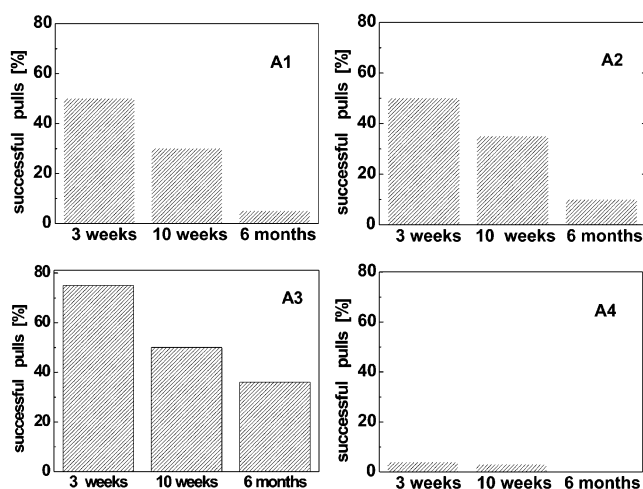


Figure 6. Fraction of successful pulls at different times.

Plateau versus Langevin Filaments. In the following, we consider the phenomenology of the successful pulls in more detail. In all cases, the statistical analysis is based on at least 60 successful pulls. We found two different scenarios for the behavior of the successfully elongated filaments. Figure 7 shows the typical evolution of mechanical parameters in the two cases, together with the corresponding static forces and the resonance frequencies.

The pattern presented in Figure 7a is seen more often. It has the following properties:

(i) During the elongation of the filament, the mechanical parameters change more or less in a stepwise manner.

(ii) Between the steps there are plateaus. On the plateaus, both the static force and the mechanical parameters remain constant.

(iii) The steps are not strictly discontinuous. The transition from one state to the next extends over a few nanometers. The plateaus are substantially longer than the transition zones. The static force curve exhibits jumps at various places at the end of the transition zone. A similar stepwise force pattern is reported in the literature.^{6,7} Following ref 6, we term this behavior “plateaulike”.

Figure 7b shows an example of the second type of evolution of the micromechanical parameters, recorded during a filament's elongation. In this case we also see steps, but between the steps there is an *increase* of the attractive force, together with an increase of the spring constant. This pattern is similar to the pattern reported in the case of elongating chains attached at both ends. This behavior is often interpreted in terms of single-chain elasticity.⁷ We call this pattern “Langevin-like”. We stress again that our pulling experiments involve mesoscale objects, not single molecules. An increase of the spring constant with extension can be caused by standard rubber elasticity. It is not characteristic of a single chain.

The ratio between the plateau and Langevin filaments depends on surface structure, that is, on aging of the film.

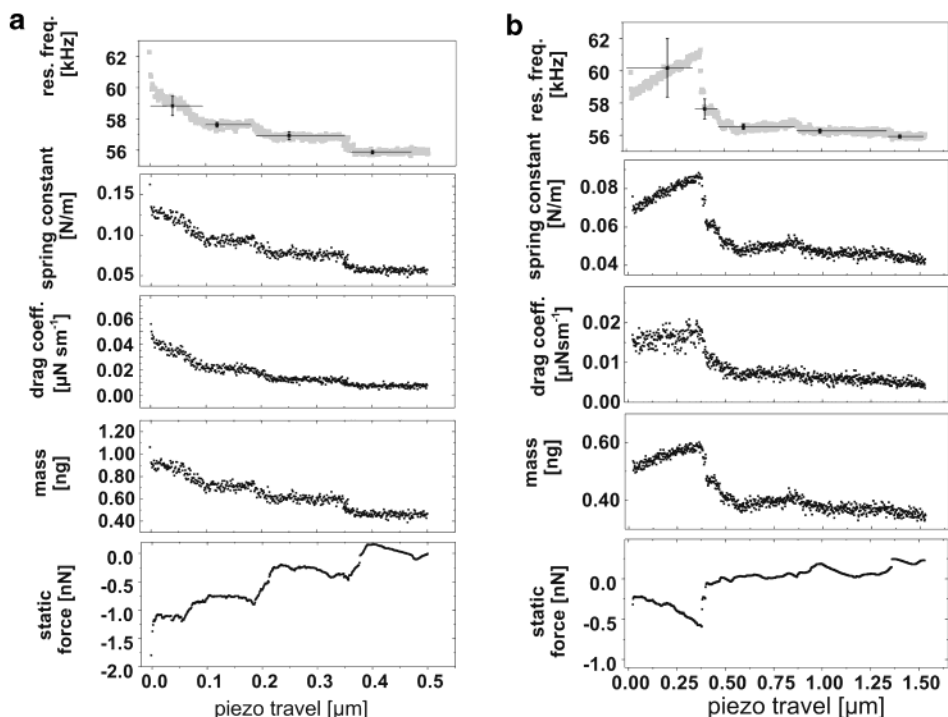


Figure 7. (a). Typical pattern of the micromechanical parameters of the system filament–cantilever in the case of a plateau filament. (b) An example illustrating the pattern of the micromechanical parameters of the system filament–cantilever–tip in the case of a Langevin filament. The piezo travel is measured relative to the closest approach to the adhesive surface (corresponding to the origin in this graph).

To distinguish between plateau and Langevin filaments on a statistical basis, we define a “plateau parameter” in the following way. For every pull, we calculate the normalized standard deviation (nSD) of the resonant frequency between two force jumps (see the top panel in Figure 7). Then we compute the average of these normalized standard deviations, obtaining a criterion which is independent of the number of transformations undergone by the particular filament. Evidently, when the resonance frequency remains constant between two steps, the nSD over each plateau is given by the experimental scatter. For Langevin objects, on the other hand, the nSD is larger because the resonance frequency evolves between two force jumps. Figure 8 shows the distribution of the plateau parameter for the systems A1, A2, and A3 three weeks after film preparation (the statistics after 10 weeks of aging is given in the Supporting Information). Clearly, the choice of the threshold value of the plateau parameter separating the plateau and the Langevin filaments is somewhat arbitrary. Since the distribution of the plateau parameter in the case of A1 is very narrow, we take this case as a reference and choose the value of 0.0053 as a limit distinguishing between plateau and Langevin filaments. According to this choice, the system A1 exhibits only plateau filaments. This criterion enables us to quantify the fraction of the plateau and the Langevin filaments as a function of aging. These data are shown in Figure 9. Note that the *total* amount of successful pulls decreases with time in all cases.

Discussion

In the following, we develop a picture which explains all our findings in a consistent way. We first summarize again our results.

- (i) The number of pulls with an extended hysteresis loop decreases with aging.
- (ii) The length of the hysteresis loop corresponds to about the particle size.

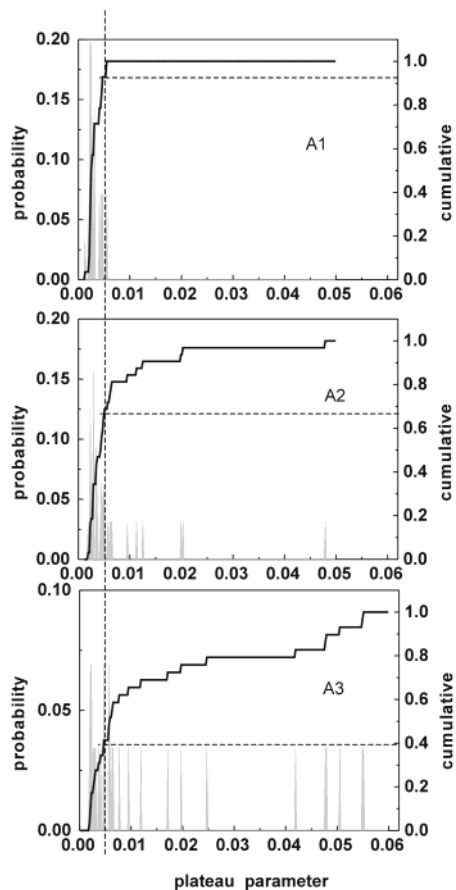


Figure 8. Distribution of the normalized standard deviation of the resonance frequency for filaments drawn from A1, A2, and A3 films. These data were obtained 3 weeks after the formation of the films. The corresponding data for 10 weeks of aging are provided in the Supporting Information.

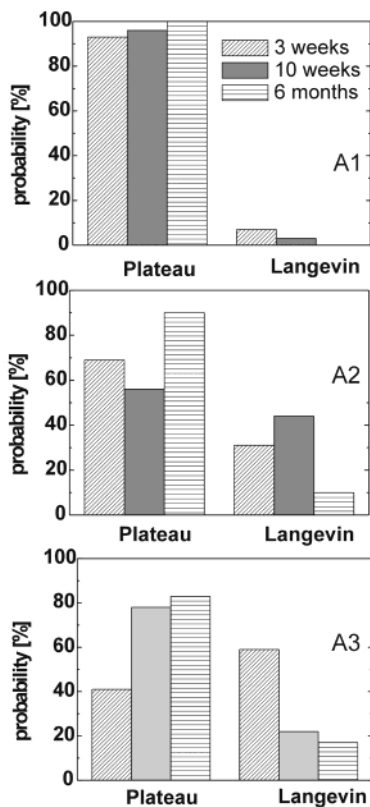


Figure 9. Fraction of the Langevin and plateau filaments for different times after film formation.

(iii) Both force curves and the evolution of the spring constant and drag coefficient are characterized by steps. Between the steps, we find either a constant force (plateau event) or forces which increase with pulling distance (Langevin event). The mechanical parameters follow the same pattern: when there is a plateau in the force, the spring constant and the friction coefficient are constant as well; when the force increases, the spring constant and the drag coefficient increase as well. Although one might think, based on intuition, that plateau filaments are better for tack, our data do not provide evidence for such a hypothesis. As Figure 8 and Figure 9 show, the most tacky material (A3) does not have a higher fraction of plateau filaments.

We explain our findings by the fact that a granular structure of the material has remained. When the particles have partially coalesced, the forces are transmitted into the medium by a finite number of bridges. In Figure 10, we provide a sketch. On the left-hand side, we show the case where the particles are softer than the continuous phase. The membranes support the stress and eventually break. On the right-hand side, we sketch a related possibility. Here the particles are stronger. The rupture occurs at the interparticle links. Both mechanisms are possible, and neither of them is necessarily assigned to plateau or Langevin events.

The steps correspond to ruptures of the bridges. It is essential for a tacky material that the number and the strength of these bridges remain sufficiently small (but nonzero, evidently). Otherwise, deformation is impossible and the tip snaps off without a hysteresis loop. For nontacky materials, the interparticle cohesion grows to the extent that filaments can no longer be pulled. One can compare the average strength of the bridges by probability histograms of the step heights (Figure 11). Both the force and the spring constant reveal that the steps on average

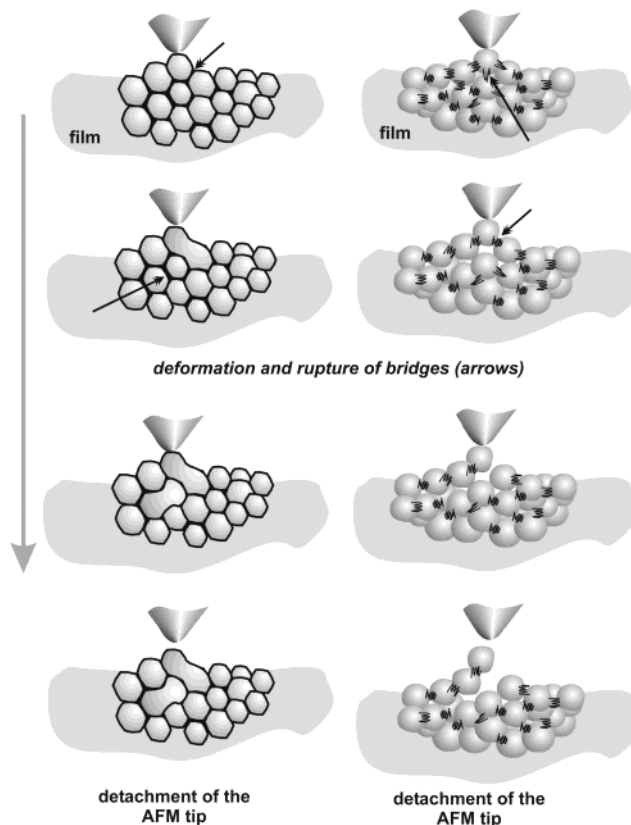


Figure 10. Two possibilities for deformation and rupture of the bridges. It is possible that interparticle links break (right-hand side). A related picture emerges if the interparticle membranes are stronger than the particles themselves. In this case, the membranes carry the stress. Under stress the membranes deform and eventually break. Note that both scenarios are possible in our systems. Neither of them is necessarily assigned to plateau or Langevin events.

are smallest for material A3, which is the most tacky material. From an engineering point of view, this finding implies that the creation of a limited amount of weak bridges will improve tack.

This leaves the question of why we see sometimes plateaus and sometimes Langevin-like force curves. Presumably, the behavior between two steps is governed by the weakest bridge. This bridge yields the most and is the one which will break next. As a general statement, a constant force always indicates that one is working against some kind of dissipative process. We associate these plateaus with contacts that do not have interdiffused chains or contacts where the connecting chains are short enough to enable viscous flow during deformation/retraction. Note that the filaments are short. Few rearrangements are needed to accommodate the formation of a filament. On the other hand, forces increasing with deformation (Langevin events) correspond to elastic behavior. If chain interdiffusion has occurred, then these connecting chains are elongated during pulling, and if they are long enough to form entanglements (if they are even branched or covalently cross-linked), then they respond elastically, producing Langevin events.

Presumably, as time proceeds more and more long chains can diffuse across particle interfaces and these interparticle boundaries grow in strength until they cannot be broken any longer. Only the contacts with limited interdiffusion remain in such a weak state. After extended aging, most of the remaining bridges are of the plateau type.

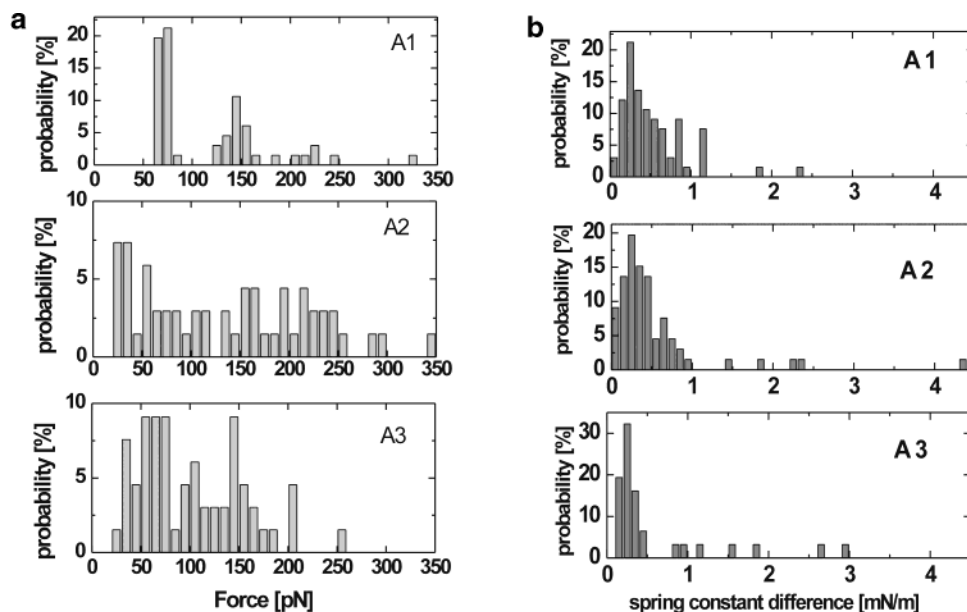


Figure 11. Distribution of (a) the jumps in the static force and (b) the differences of the spring constant over two neighboring plateau events.

Conclusions

We have studied the fibrillation process of films of polyacrylic pressure sensitive adhesives on the macroscopic and mesoscopic scales. The energy of separation as measured with a macroscopic tack tester was correlated to the likelihood of drawing mesoscopic filaments. The analysis of the Brownian motion of the cantilever allowed for *in situ* local mechanical measurements on the tip-sample contact.

Both the macroscopic energy of separation and the fraction of successful pulls correlate with incomplete film formation as evidenced by the AFM micrographs. The hysteresis loops observed when pulling filaments are characterized by discrete steps, which we assign to the rupture of interparticle junctions. As the film ages, these junctions become more and more tight. Tacky materials retain their ability to form filaments. A granular structure with weak interparticle junctions is beneficial for tack.

Between the steps, the phenomenology of the hysteresis loops is variable. We sometimes find extended plateaus in both static force and spring constant. Again, the plateaus are most often observed for tacky materials.

Tack requires a delicate balance between adhesive tip-sample forces and cohesive forces inside the sample. A granular structure with a limited number of interparticle links can improve tackiness.

Acknowledgment. One of us (T.D.D.) has been supported by a Marie Curie Fellowship of the European Community program "Human Potential" under Contract Number HPMF-CT-2001-01188 and partially by "Laboratoires Européens Associés" (LEA) on Polymers in Confined Geometries between the MPI for Polymer Research, Mainz, and CNRS-ICS, Strasbourg.

Supporting Information Available: Sketch of the experimental configuration employed for filament elongation; distribution of the average standard deviation of the resonance frequency for filaments drawn from A1, A2, and A3 films, 10 weeks after the formation of the films; feedback parameters for AFM imaging. This material is available free of charge via the Internet at <http://pubs.acs.org>.

LA0300232